Progress In Electromagnetics Research C, Vol. 51, 121–129, 2014

Fractal-Based Triangular Slot Antennas with Broadband Circular Polarization for RFID Readers

Jianjun Wu*, Xueshi Ren, Zhaoxing Li, and Yingzeng Yin

Abstract—Equilateral-triangular slot antennas with modified edges for wideband circular polarization are proposed in this paper. Circular polarization was firstly obtained by adding two asymmetric perturbations to two edges of triangular slot. Then fractal-like boundaries were adopted in the antenna design for size reduction and broadband operation. Two antenna prototypes for RFID readers were fabricated to cover RFID UHF band and ISM 2.4 GHz band, respectively. Measured results show that the presented antennas obtain fairly wide 3-dB axial ratio bandwidths of 15.7% (820–960 MHz) and 19.8% (2.18–2.66 GHz).

1. INTRODUCTION

Recently, radio frequency identification (RFID) technology has been applied to numerous areas such as retail industries, asset identification, animal tracking and vehicle security. RFID systems operate at widely differing frequencies, ranging from 125 kHz to 5.8 GHz in the microwave range. Various RFID applications can be found in the ultra high frequency (UHF) band ranging from 840 to 960 MHz and the industrial-scientific-medical (ISM) band from 2.4 to 2.5 GHz due to their long readable range and fast reading speed [1]. As is known to all, the RFID reader antenna is an important component in RFID systems and is often designed with circularly polarized (CP) behavior, because CP antennas allow flexible orientations between the reader and the tag antenna [2]. Taking the two aspects into account, designing CP antennas across wide operating bands is a significant issue for RFID reader antennas. Moreover, small antenna size is also required in RFID handheld readers.

To obtain wideband circular polarization, slot antennas such as ring slot [3, 4], and square slot [5–7], are often used because of their low quality factors due to bidirectional radiation characteristics. Note that CP waves can be yielded when perturbation structures are embedded in the slots with $\pm 45^\circ$ away from the feeding lines. In [8], a combination of positive and negative perturbations is adopted in the dual layer rings to broaden axial ratio (AR) bandwidth, in which positive perturbation refers to cutting corners of the ring while negative perturbation extending corners. On the other hand, in compact antenna designs, triangular patches have smaller sizes as compared to square and circular patches [9–11]. By cutting a small triangle from the triangle edge [9], loading turning stub at triangular tip [10], or inserting near semicircular notch into the edge [11], CP radiations are achieved. But narrow AR bandwidth of 2.3%, 1.03% and 3% are obtained respectively. Combining these two points of view, triangular slots are good candidates for broadband and compact CP antennas. Nowadays, fractal shaped antennas have been proposed for wideband and compact applications because of their interesting features [12–14]. In [12], a semi-Spidron fractal is utilized in a right-angled triangle slot. By merging downscaled copies of a right-angled triangle slot, a 3-dB AR bandwidth of 15.2% is achieved. Fractals are adopted in CPW structure [13] to obtain circular polarization with AR band from 900 to 936 MHz (4%). Slots with fractal boundaries are proved to have a small dimension [14] due to the fact that fractal

Received 25 May 2014, Accepted 19 June 2014, Scheduled 23 June 2014

* Corresponding author: Jianjun Wu (jun542391752@126.com).

The authors are with the Science and Technology on Antenna and Microwave Laboratory, Xidian University, Xi'an, Shaanxi 710071, People's Republic of China.

provides longer current path. But the antenna in reference [14] only focuses on linear polarization and near-field radiation.

The goal of this paper is to obtain a wide CP bandwidth with compact antenna size. The CP operation is realized by asymmetry perturbations and the techniques of triangular slot and fractal-like boundaries are adopted for size reduction. The presented wide band CP antennas are designed for UHF and 2.4 GHz RFID readers respectively. Details of the antenna design and experimental results are demonstrated.

2. DESIGN PROCEDURE AND ANALYSIS

Figure 1 shows the geometry of the proposed slot antenna and the design evolution process is displayed in Figure 2. By adding a triangle to one edge of the equilateral-triangular slot antenna 1, antenna 2 is designed for CP characteristic. A disk is attached to the open-ended feeding line to match the impedance. A smaller triangle is cut from another triangular edge and antenna 3 is formed. Taking the concept of fractal, the edges of the two perturbations are further modified to reduce the antenna's size in antennas 4. Antennas 2 to 4 are designed to operate around 2.4 GHz. Antenna 2 and 3 have the same ground length $G = 60$ mm and $G = 50$ mm in antenna 4. All the slot antennas are designed on FR4 dielectric substrate that has dielectric constant of 4.4, loss tangent of 0.02 and thickness $H = 1$ mm. The optimized parameters and simulated results are carried out with the aid of Ansoft HFSS 13.0 software and detailed design process and analysis are discussed below.

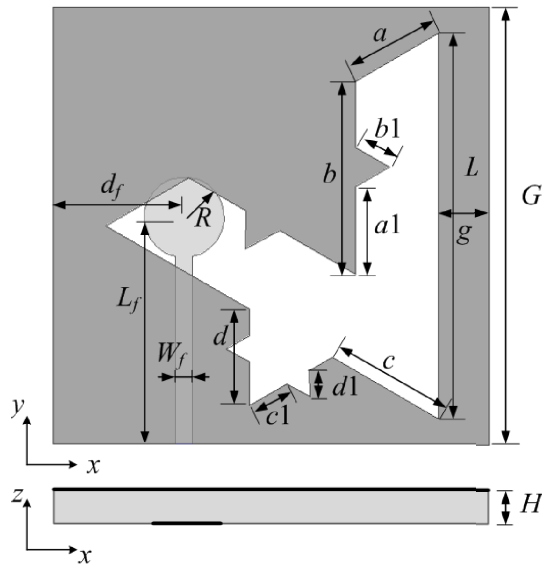

Figure 1. Geometry of the proposed antenna.

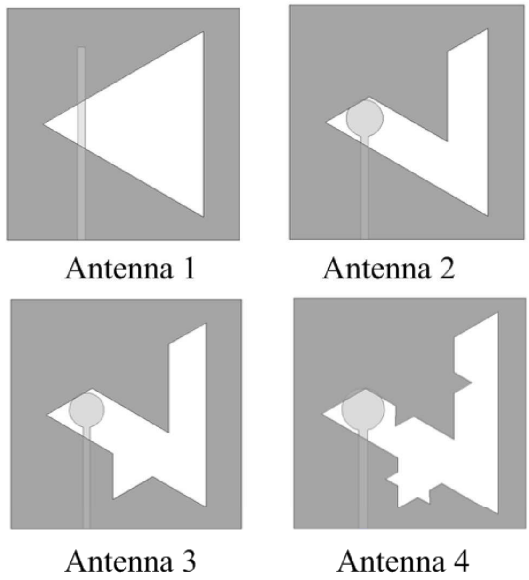

Figure 2. Antenna design evolution process.

2.1. Design of Antenna 3 with Combined Perturbations

Like the V-shaped patch in reference [9], an equilateral triangle is added to the upper edge of the slot antenna 1 to achieve CP radiation. In antenna 3, another triangle is cut from the lower edge to further improve the bandwidth due to the fact that adding triangle can be seen as negative perturbation, while cutting triangle as positive perturbation, just as studied in [8]. As seen in Figure 3, resonant mode 1 with higher frequency is yielded between the adding triangle tip and bottom right tip and lower mode 2 between the cutting triangle tip and the upper right tip. The two modes have $\pm 45^\circ$ phase difference from the feeding disc respectively and then 90° phase difference is generated between the two orthogonal modes, as E-field distributions shown in Figure 3. Mode 1 has phase 90° ahead of mode 2 and then right-hand circular polarization (RHCP) is yielded in $+z$ direction. Polarization of RHCP can

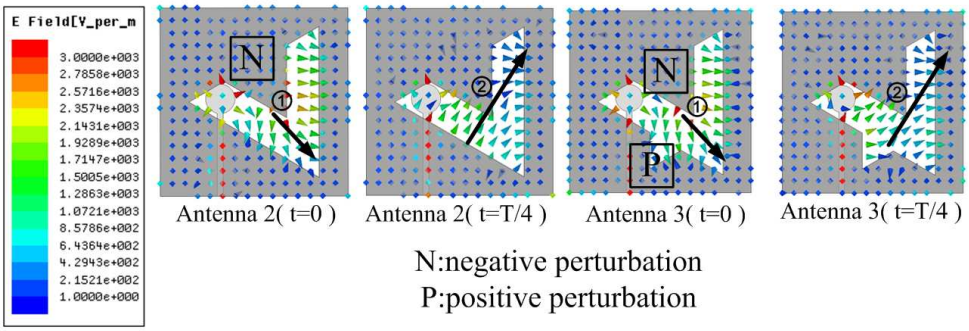

Figure 3. *E*-field distributions of antennas 2 and 3 in a quarter cycle.

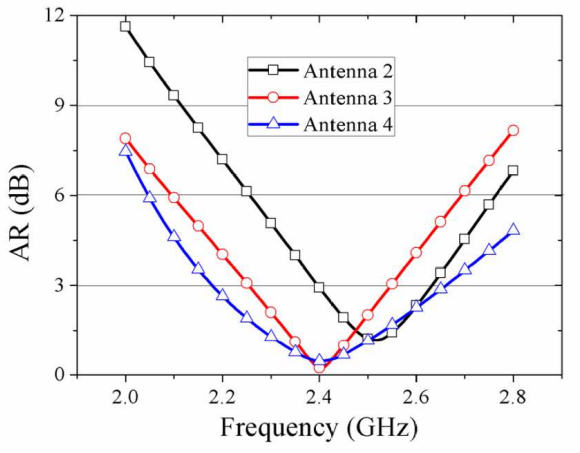

Figure 4. Axial ratio curves for antennas 2 to 4.

be changed to left-hand circular polarization (LHCP) when the negative perturbation is added to lower slot edge and positive perturbation to upper edge.

The optimized parameters for antenna 3 are $G = 60\,\text{mm}$, $L = 48\,\text{mm}$, $g = 9.2\,\text{mm}$, $a = 11.2\,\text{mm}$, $b = 23\,\text{mm}$, $c = 16\,\text{mm}$, $d = 12\,\text{mm}$, $W_f = 1.9\,\text{mm}$, $L_f = 31.3\,\text{mm}$, $R = 4.5\,\text{mm}$, and $d_f = 19.7\,\text{mm}$. It is demonstrated in [15] that the resonant frequency for an equilateral triangular patch operating at TE_{10} mode is,

$$f = \frac{2c}{3a\sqrt{\varepsilon_{eff}}} \tag{1}$$

$$\varepsilon_{eff} \approx \frac{\varepsilon_r + 1}{2} \tag{2}$$

where c is the speed of light, a is the length of the equilateral triangle edge, ε_r is relative permittivity of substrate and ε_{eff} is the effective relative permittivity in consideration of substrate in free space. In our antenna, ε_{eff} is approximately equal to 2.7 corresponding to the FR4 substrate with relative permittivity of 4.4. The calculated resonant frequency is 2.54 GHz for triangular slot antenna 1. In antenna 3, two resonant frequencies of approximate 2.27 GHz and 2.92 GHz are calculated for the two modes. Consequently, good CP characteristics can be obtained between the two frequencies, which are in good agreement with simulated results.

The simulated AR curves for antennas 2 and 3 are shown in Figure 4. The 3-dB AR bands are 2.4–2.63 GHz (9.0%) for antenna 2 and 2.24–2.55 GHz (12.9%) for antenna 3, which have been tabulated in Table 1. The result that AR band moves to lower frequency can be explained that the lower resonant frequency decreases when the triangle is cut from antenna 2 since the distance between the cutting triangle tip and the upper right tip is increased.

Table 1. AR bandwidths of antennas 2 to 4.

Antenna	Antenna size (mm^2)	3-dB AR bandwidth
2	60×60	9.0%
3	60×60	12.9%
4	50×50	19.8%

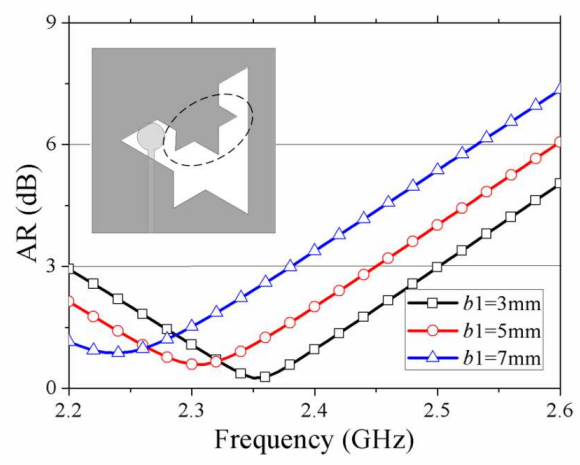

Figure 5. Effect of b_1 on AR.

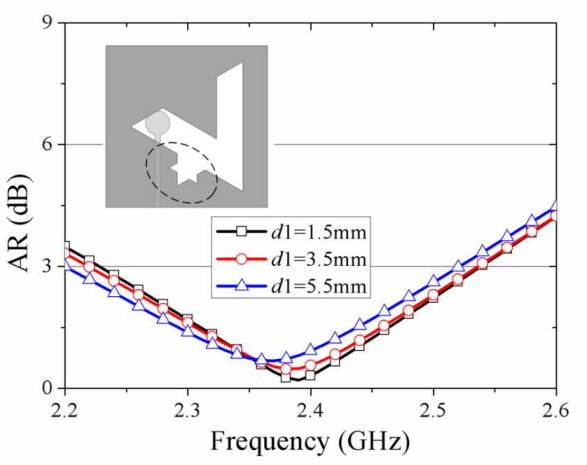

Figure 6. Effect of d_1 on AR.

2.2. Design of Antenna 4 with Fractal-like Edges

It is demonstrated in [14] that the Koch Fractal used in triangular slot can include more electrical length inside a fixed physical space. Thus a smaller antenna size is obtained by employing fractal boundaries. Figure 5 and Figure 6 show the effects of the dimensions of the upper and lower fractals on the AR characteristics. It is obviously that larger fractal dimension results in lower AR centre frequency because they can provide longer current path. And the upper fractal exhibits a fiercer impact on AR than the lower fractal since the upper fractal has larger area. It is noteworthy that because the locations and dimensions of the small triangles are arbitrary in our design, which is not strictly in accordance with the fractal rules, the structure proposed in this paper can be called as fractal-like boundaries.

Antenna 4 is designed to operate around 2.4 GHz on the basis of antenna 3. Antenna 4 has a smaller ground $G = 50\,\text{mm}$ and the other parameters are $L = 44\,\text{mm}$, $g = 6\,\text{mm}$, $a = 11\,\text{mm}$, $b = 22\,\text{mm}$, $c = 14\,\text{mm}$, $d = 11\,\text{mm}$, $a_1 = 10\,\text{mm}$, $b_1 = 4.5\,\text{mm}$, $c_1 = 5\,\text{mm}$, $d_1 = 3\,\text{mm}$, $W_f = 1.9\,\text{mm}$, $L_f = 26\,\text{mm}$, $R = 4.6\,\text{mm}$, and $d_f = 12\,\text{mm}$. The simulated AR bandwidth for antenna 4 is 19.8% (2.18–2.66 GHz). Antenna 4 will have a lower center frequency than antenna 3 when only fractal-like edges are added. And the antenna's size can be reduced when the antenna is tuned to operate at 2.4 GHz. Wider AR band for antenna 4 can also be seen as compared to antenna 3.

2.3. Effects of Feeding Line on Impedance Matching and Radiation Performance

The feeding structure consists of a circular disk and microstrip feeding line. By adjusting the dimension and position of the disk, good impedance matching can be achieved. Figure 7 shows the effects of disk position on antenna input resistance and AR. Larger resistance values can be observed when feeding point is moved away from the slot center along x-axis and varied near the slot center along y-axis, which is similar to the impedance of conventional patch antenna. Parameter d_f affects the center frequency of AR band while L_f influences AR curve slightly. The effects of disk radius R on antenna's performance are shown in Figure 8. It can be seen that radius R has little affection on the CP characteristic. But when R is tuned from 3.6 mm to 5.6 mm, the lowest point of $|S_{11}|$ curve drops to lower frequency. Different

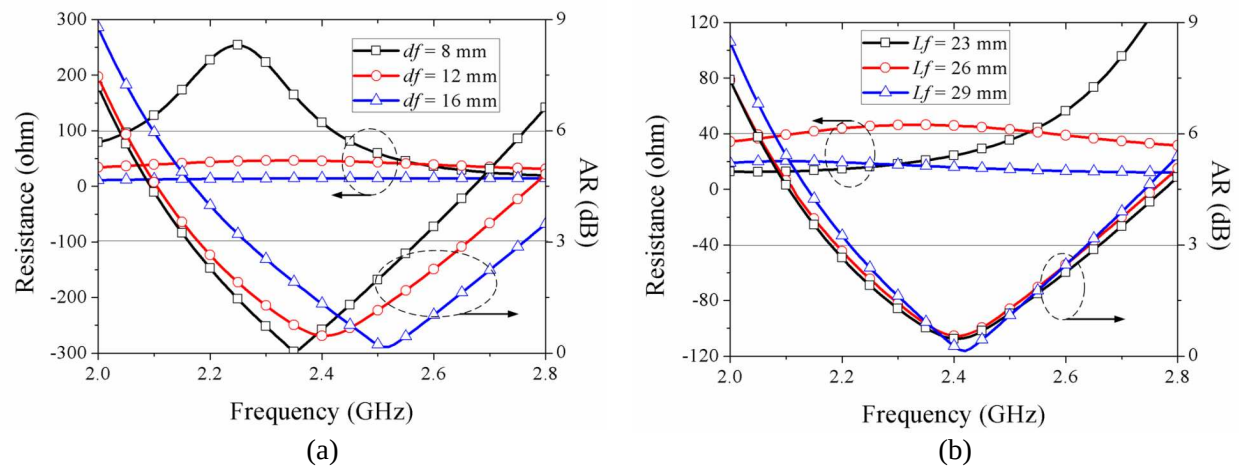

Figure 7. Effects of feeding position of (a) d_f and (b) L_f on input resistance and AR.

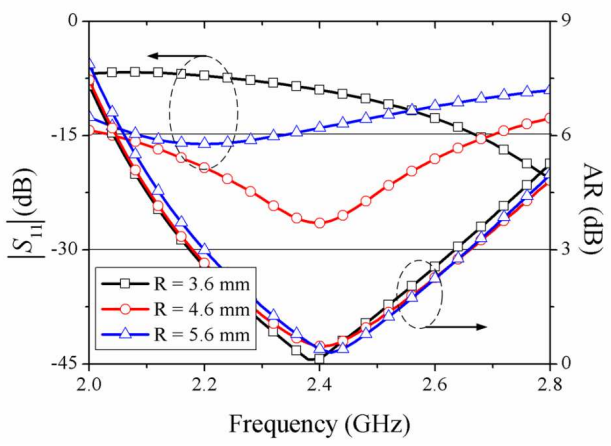

Figure 8. Effects of disc radius R on $|S_{11}|$ and AR.

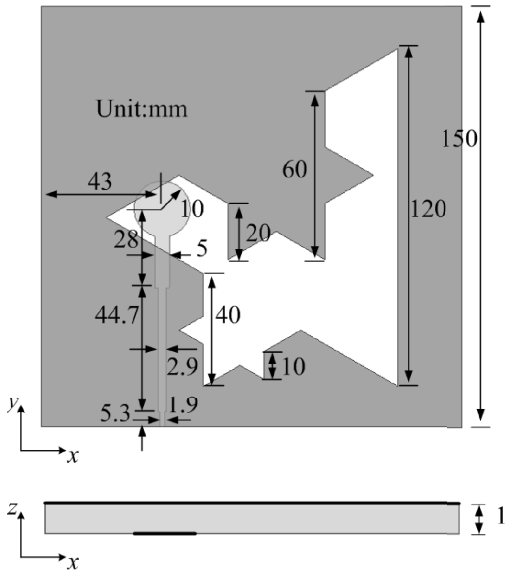

Figure 9. Dimensions of antenna 5 operating at UHF band.

R values provide different capacities and impedance conversions and minimum of $|S_{11}|$ is -26 dB at 2.4 GHz when R is 4.6 mm. From the parameters analyses above, it is found that feeding line plays an important role in impedance matching. Feeding position d_f is tuned together with slot parameters to obtain good CP radiations. Since the patterns of slot are bidirectional and determined mainly by slot form, feeding line has little influence on radiation patterns, for example, the patterns for theta angle larger than 90°. Additionally, wide impedance bandwidth can be achieved by the combination of disk and feeding line instead of merely single microstrip line.

2.4. Design of Antenna 5 Operating at UHF Band

Since UHF RFID applications in different countries have different spectrum reserved, such as 865–869 MHz in Europe, 902–928 MHz in USA, 840.5–844.5 MHz and 920.5–924.5 MHz in China, Antenna 5 is designed to operate over the universal band ranging from 840 to 960 MHz. Antenna 5 has the same operating mechanism as Antenna 4. The optimized parameters for Antenna 5 are showed in Figure 9.

A stepped impedance transformer is adopted to the feeding line.

To give detailed design principles of the proposed fractal-based slot antennas, simple design steps are summarized as follows:

Step 1) Create an equilateral triangular slot according to Equations (1) and (2) on the basis of operating frequency and substrate parameters.

Step 2) Add perturbations to the slot edges. The size of the upper added triangle is about half of the slot and the lower cut one is about one third of slot edge.

Step 3) Apply fractal edges to perturbations and decrease the slot size to adjust AR center frequency.

Step 4) Insert disk to feeding line for impedance matching by tuning the position and size of disk.

3. MEASURED RESULTS

To validate the design strategies, antenna 4 and antenna 5 were fabricated and the photographs are shown in Figure 10. Measured S parameters were achieved by using Agilent N5062A Vector Network Analyzer. Radiation characteristics including RHCP and LHCP patterns were measured in an anechoic chamber with SATIMO system. Figure 11 shows the measured and simulated $|S_{11}|$ and AR along $+z$-axis of antenna 4 and antenna 5. For antenna 4, the measured 10-dB $|S_{11}|$ band is from 1.72 to 3.08 GHz (26.8%) and 3-dB AR band is from 2.17 to 2.66 GHz (19.8%). Wide impedance bandwidth is obtained by the disk-ended feeding mechanism. For antenna 5, the measured 10-dB $|S_{11}|$ bandwidth is of 28.9% (740–990 MHz) and 3-dB AR bandwidth is of 15.7% (820–960 MHz). Good agreements are

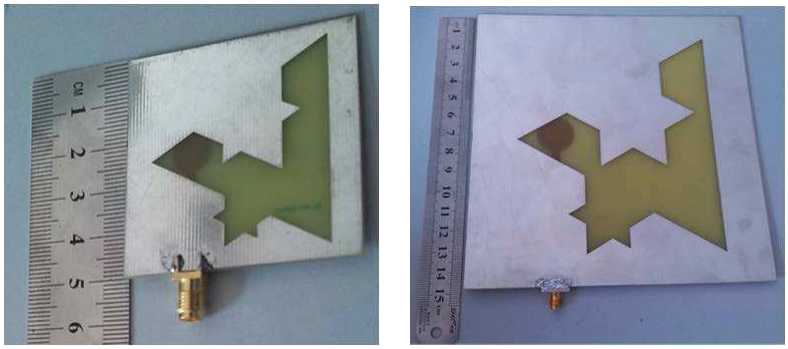

(a) (b)

Figure 10. Photographs of fabricated (a) antenna 4 and (b) antenna 5.

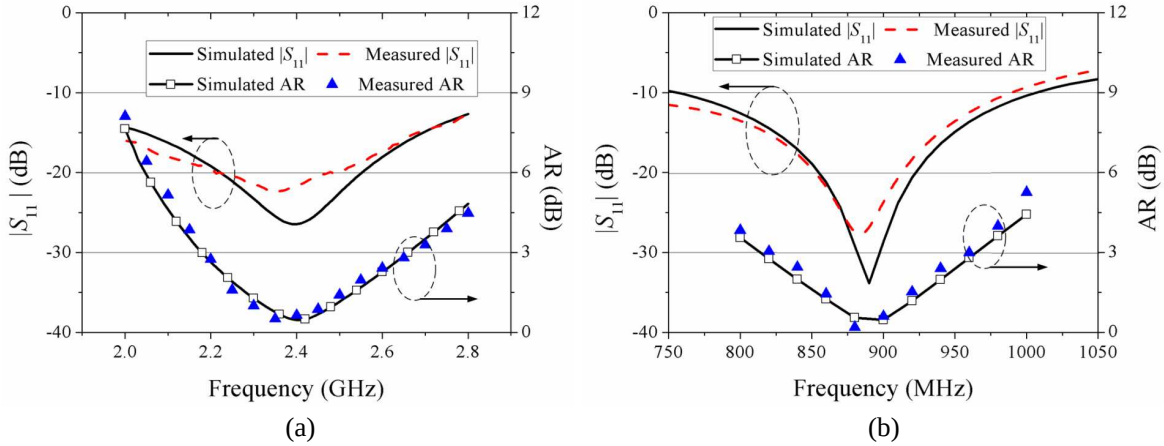

Figure 11. Simulated and measured $|S_{11}|$ and AR of (a) antenna 4 and (b) antenna 5.

observed between the simulated and measured results. The simulated and measured radiation patterns for the two antennas are presented in Figure 12. The radiation patterns are bidirectional and RHCP is obtained in the upper-half plane. Antenna 4 has 3-dB AR beam widths of 90° and 100° in two principal planes (*xoz*-plane and *yoz*-plane) and 60° and 90° for antenna 5. Figure 13 depicts the measured gains along $+z$-axis against frequency for the two antennas. Antenna 4 shows stable gains within the effective

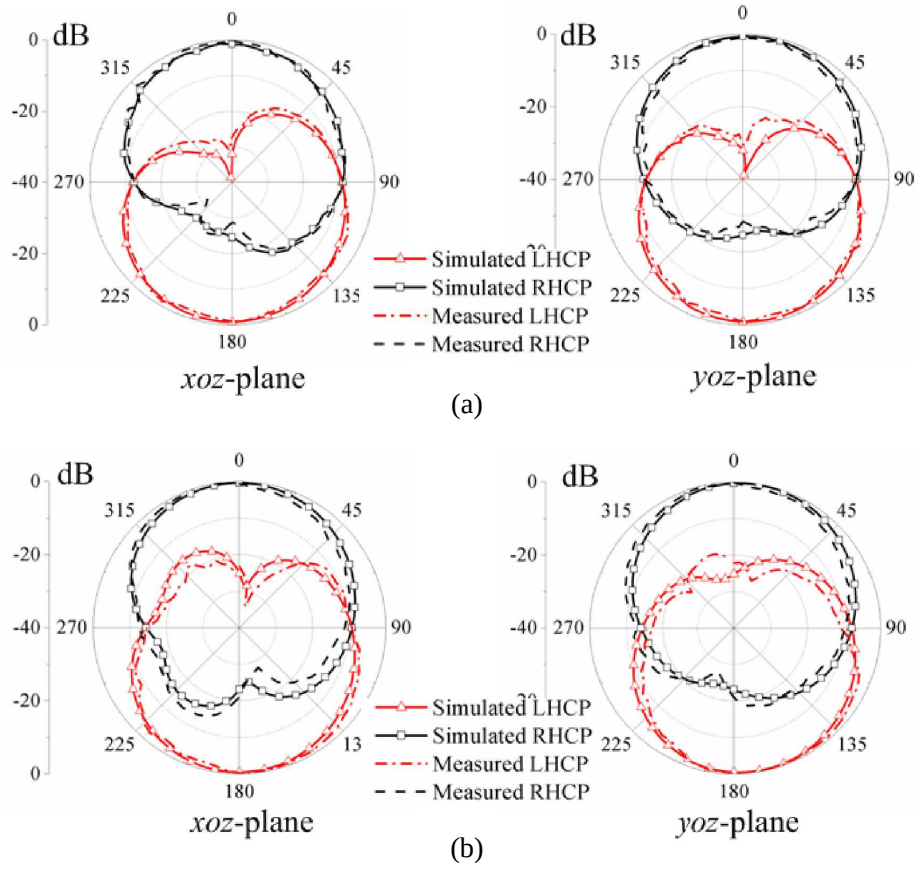

Figure 12. Simulated and measured radiation patterns of (a) antenna 4 at 2.4 GHz and (b) antenna 5 at 900 MHz.

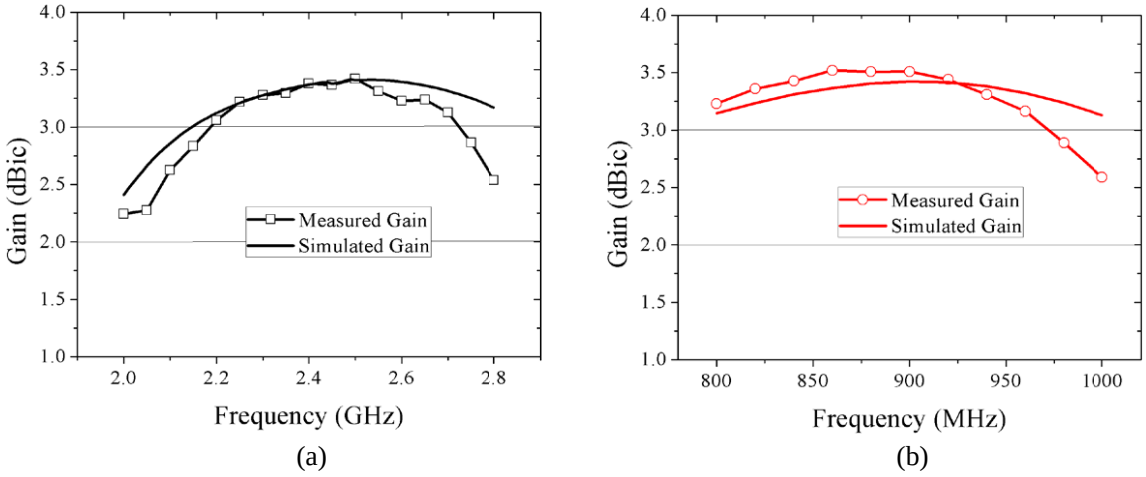

Figure 13. Simulated and measured gains of (a) antenna 4 and (b) antenna 5.

Table 2. Comparison between proposed and reference antennas.

References	Antenna Size	3-dB AR CP bandwidth
3	$0.47\lambda_0 \times 0.47\lambda_0$	10.5%
4	$0.46\lambda_0 \times 0.46\lambda_0$	8.1%
5	$0.57\lambda_0 \times 0.57\lambda_0$	12.4%
6	$0.39\lambda_0 \times 0.38\lambda_0$	17.7%
7	$0.29\lambda_0 \times 0.29\lambda_0$	8.7%
12	$0.57\lambda_0 \times 0.57\lambda_0$	15.2%
13	$0.28\lambda_0 \times 0.32\lambda_0$	4%
Proposed antenna 4 @ 2.4 GHz	$0.4\lambda_0 \times 0.4\lambda_0$	19.8%
Proposed antenna 5 @ 900 MHz	$0.45\lambda_0 \times 0.45\lambda_0$	15.7%

AR bands with a peak gain of 3.6 dBic at 2.4 GHz. Antenna 5 exhibits the measured gain of more than 3 dBic over the band of 840–960 MHz.

Table 2 shows the comparison of antenna sizes and performance between antennas in references and proposed antennas. Note that all the listed antennas are of bidirectional radiation and λ_0 is the wavelength in free space corresponding to center working frequency of each antenna. It can be seen that the proposed triangular slots achieve wide AR bandwidths but occupy small dimensions.

4. CONCLUSION

Triangular slot antennas with modified edges for broadband circular polarization are presented in this paper. Asymmetry perturbations are added to the slot edges to obtain wide CP bandwidth. By adopting fractal-like boundaries, AR band is further broadened and antenna size is reduced simultaneously. The measured results show that two antenna prototypes can cover UHF band from 840 to 960 MHz and ISM band from 2.4 to 2.5 GHz, respectively. In addition, the antenna structure is simple and easy to fabricate which makes it good candidate for RFID readers.

ACKNOWLEDGMENT

This work is supported by the Fundamental Research Funds for the Central Universities (Grant No. K5051302035).

REFERENCES

1. Finkenzeller, K., *RFID Handbook*, 2nd Edition, Wiley, New York, 2003.
2. Lin, Y.-F., C.-H. Lee, S.-C. Pan, and H.-M. Chen, "Proximity-fed circularly polarized slotted patch antenna for RFID handheld reader," *IEEE Transactions on Antennas and Propagation*, Vol. 61, No. 10, 5283–5286, 2013.
3. Sze, J.-Y., C.-I. G. Hsu, M.-H. Ho, Y.-H. Ou, and M.-T. Wu, "Design of circularly polarized annular-ring slot antennas fed by a double-bent microstripline," *IEEE Transactions on Antennas and Propagation*, Vol. 55, No. 11, 3134–3139, 2007.
4. Zhang, J. L. and X. Q. Yang, "Integrated compact circular polarization annular ring slot antenna design for RFID reader," *Progress In Electromagnetics Research Letters*, Vol. 39, 133–140, 2013.
5. Chou, C. C., K. H. Lin, and H. L. Su, "Broadband circularly polarised cross-patch-loaded square slot antenna," *Electronics Letters*, Vol. 43, No. 9, 485–486, 2007.
6. Lu, J.-H. and S.-F. Wang, "Planar broadband circularly polarized antenna with square slot for UHF RFID reader," *IEEE Transactions on Antennas and Propagation*, Vol. 61, No. 1, 45–53, 2013.

7. Lin, Y.-F., H.-M. Chen, F.-H. Chu, and S.-C. Pan, "Bidirectional radiated circularly polarised square-ring antenna for portable RFID reader," *Electronics Letters*, Vol. 44, No. 24, 1383–1384, 2008.
8. Latif, S. I. and L. Shafai, "Circular polarization from dual-layer square-ring microstrip antennas," *IET Microwaves, Antennas and Propagation*, Vol. 6, No. 1, 1–9, 2012.
9. Rasheed, A. A. and G. Kumar, "Single feed circularly polarized modified triangular microstrip antennas," *Antennas and Propagation Society International Symposium*, Vol. 2, 818–821, 1994.
10. Lu, J.-H. and K.-L. Wong, "Single-feed circularly polarized equilateral-triangular microstrip antenna with a tuning stub," *IEEE Transactions on Antennas and Propagation*, Vol. 48, No. 12, 1869–1872, 2000.
11. Yeh, C. H., Y. W. Hsu, and C. Y. D. Sim, "Equilateral triangular patch antenna for UHF RFID applications," *International Journal of RF and Microwave Computer-Aided Engineering*, 2014, Doi: 10.1002/mmce.20801.
12. Hwang, K. C., "Broadband circularly-polarised Spidron fractal slot antenna," *Electronics Letters*, Vol. 45, No. 1, 3–4, 2009.
13. Raviteja, C., C. Varadhan, M. Kanagasabai, A. K. Sarma, and S. Velan, "A fractal-based circularly polarized UHF RFID reader antenna," *IEEE Antennas and Wireless Propagation Letters*, Vol. 13, 499–502, 2014.
14. Pakkathillam, J. K., M. Kanagasabai, C. Varadhan, and P. Sakthivel, "A novel fractal antenna for UHF near-field RFID readers," *IEEE Antennas and Wireless Propagation Letters*, Vol. 12, 1141–1144, 2013.
15. Dasgupta, S., B. Gupta, and H. Saha, "Compact equilateral triangular patch antenna with slot loading," *Microwave and Optical Tehcnology Letters*, Vol. 56, No. 2, 268–274, 2014.